DISCUSSION ON SCALE EFFECT IN DYNAMIC FRAGMENTATION

I. V. Simonov[1] and N. Pugno[2]
[1]Institute for Problems in Mechanics RAS, 119526 Moscow,Russia, simonov@ipmnet.ru
[2]Department of Structural Engineering, Politecnico di Torino,
Corso Duca degli Abruzzi 24, 10129, Torino, Italy, n-pugno@polito.it

ABSTRACT

The dynamic large-scale fragmentation resulting in a large impact or explosion is discussed. It is known that, unlike the lab-scale tests and independently on the type of explosion, energy and so on, the fragment size distribution presents maximums explained by block structure of the rocks and that this number grows with increasing the fragment size. A *quantum-continuous model* for this distribution in a rock cell under the long-length primary wave action is proposed. Thus, the differential and cumulative distributions over the whole fragmentation volume are calculated, and the free-parameters in the model are fitted to the experimental data.

INTRODUCTION

Fragmentation of solids involves many natural and artificial processes, ranging from sky body collisions to comminution of coffee grains. Such phenomena play an important role in the formation of various structures (asteroid clouds, impact/explosion craters, etc.) and are distinguished by diversity, dependence on many factors and complexity of description. Fundamental investigations in this area began from lab-scale tests in statics [1-3] -see [4] - and later in dynamics [5,6]. Their findings serve as the basis firstly for empirical laws and then for theoretical predictions. Assuming the fractal law for the size distribution of particles, Carpinteri and Pugno [7,8] have unified the three comminution laws proposed by von Rittinger [1], Kick [2] and Bond [3] for predicting the energy consumption in fragmentation. A theoretical model [7] was followed by some experiments on drilling and compression of heterogeneous materials [8]. They also confirm the fractal nature of fragmentation and lead to the determination of the model parameters. In dynamics, the stone ball fracture resulting in impact by a projectile at 0.1-3 km/s shows that the distribution is subject to the same law, but it is described inserting two distinct fractal dimensions. The last peculiarity was later explained by a geometrical feature of the primary wave propagation inside the ball [9], where, based on the continuum damage theory of dynamic fragmentation developed by Grady and Kipp [10], the thorough computer-analytic simulation appears to be in a good agreement with the lab-scale impact experiments. Note that Carpinteri and Pugno [8] found the same result in perforations: the bi-fractality was explained as due to two different fracture mechanisms under the drilling tool, namely, cutting and crushing.

However, all these experiments were performed only at the micrometer fragment size range. Meantime, it was repeatedly noted that the scale effect is of great importance in fragmentation. As a matter of fact, the fragment size distribution observed after many large explosions (to kilotons energy) in rocks, does not follow the simple (mono) fractal law in the range 1-100 cm [11]. Unlike the small-scale tests, it has maximums explained by the block structure of rocks and moreover, the number of pieces surprisingly grows when the fragment size increases. These peculiarities only slightly depend on the type of explosion, its energy, and the depth of the charge laying.

To describe all scales of dynamic fragmentations resulting in a large impact or explosion in this work, we suggest a *quantum-continuous model* of the local fragmentation distribution using the evidence on how the primary wave traveling through a cell of the rock spends its energy into fracture and heat, as recently emphasized by Simonov [12]. For the finer fragmentation (<5 mm), Melosh's et al. description is adopted [9]. When changing to the block fracture with a hierarchy of characteristic sizes, the degenerate distribution function, that presents singularities, is inserted into the model. By integrating the local distributions, the global distribution over the whole destroyed volume is found out. Forcing the free model parameters to fit the empirical data [11] leads to remarkable agreement between theory and observations. Nevertheless, the restriction of the empirical data concerning quantity and accuracy, as well as the usual incorrectness of the similar reverse problems, leave behind them a great deal with concerning the possibility of refining the present simulation.

PHYSICAL ASUMPTIONS

Consider the fragmentation resulting in a large (sub)surface blast or collision of a massive projectile with a large-size brittle solid body simulated by an elastic half-space. Assume that the semi-spherical primary wave propagates starting at the distance R_0, a conventional radius from the point of action, and with initial magnitude in mass velocity $U_0 = 3.69\,\mathrm{km/s}$, where the imaginary melting/solid boundary takes place according to reference [12]. Then, a description of the shock wave propagation for accounting the thermodynamics, in particular, its specific energy lost $f(r)$ - the energy spent to destroy a cell of $1\mathrm{m}^3$ - will be identical to as reported in [12]. So, the wave, emerged by a large action, propagates according to the well-known empirical law in dependence on dimensionless coordinate $r = R/R_0$ with the decay coefficients, α ($U_0 > U > U_1$, $U_1 \approx 30\,\mathrm{m/s}$) and β ($U < U_1$) at stages of strong and weak shock wave, respectively (typically α =1.87 and β =1.6 for rocks [13, 14]). The radius R_0 and wave width, H, can be evaluated from the experimental data [13] and thus it follows that $R_0 \approx 4.2\mathrm{m}$ and $H \approx 20 - 30\mathrm{m}$ for the 5 kilotons TNT explosion in granite, so that we choose $H/R_0 = 5$ for the future calculations.

In the domain of the fine fragmentation, we employ the differential distribution of particle sizes over a cell given in reference [9]:

$$p_c(l,r) = A_0 l_{\max}^{-4} L^3 (1-L)^{m-1}, \quad L = l/l_{\max} \tag{1}$$

where $p_c(l)\mathrm{d}l$ is the number of particles per $1m^3$ with sizes between l and $l + \mathrm{d}l$, $l_{\max}$ is the peak size, A_0 is the normalizing constant and *m* is a free parameter ($m \le 10$). This is valid for $l < 5\mathrm{mm}$. If $l \ge 5\mathrm{mm}$, the characteristic sizes of the block structure of various rocks ($l_1 = 5,\quad l_2 = 20,\quad l_3 = 50,\quad l_4 = 140,\quad l_5 = 500,\quad l_6 = 1000\mathrm{mm}$), play a fundamental role in fragmentation: they determine maximums in the numbers of pieces with respect to the size [11]. Thus, when $l_j < l < l_{j+1}$ we advance the following degenerate distribution $p_c(l,r)$:

$$p_c = A_1 g(l), \quad l_{\min} = l_j \le l \le l_{\max} < l_{j+1}, \quad r_{n-1} < r < r_n, \quad n = 3j \tag{2a}$$

$$p_c = A_2 s(l) + A_3 g(l), \quad l_j \le l \le l_{j+1} = l_{\max}, \quad r_n < r < r_{n+1} \tag{2b}$$

$$p_c = A_4 s(l), \quad l_j < l_{\min} \le l \le l_{j+1}, \quad r_{n+1} < r < r_{n+2} \tag{2c}$$

$$g(l) = l_j^{-4}\left(\frac{l_{j+1} - l}{l_{j+1} - l_j}\right)^{m_j}, \quad s(l) = l_{j+1}^{-4}\left(\frac{l - l_j}{l_{j+1} - l_j}\right)^{m_j}, \quad j = 1,...,J \qquad \text{(2e)}$$

For us J=8 due to $l_7 = 2000,\ l_8 = 3000$ mm are added as the imaginary maximums, and m_j are free parameters in the considered scale-range.

To determine the pairs $(A_1, l_{\max})$, (A_2, A_3) and $(A_4, l_{\min})$ as functions of *r*, we have the condition that the sum of individual volumes equals $1\mathrm{m}^3$, and the energy balance equation:

$$\int_{l_{\min}}^{l_{\max}} l^3\ p_c(l,r)dl = 1, \quad f(r) = \int_{l_{\min}}^{l_{\max}} GK(l)\ p_c(l,r)dl, \quad K(l) = K_0 l^{-k} \qquad (3)$$

where $G \approx 20\,\mathrm{J/m^2}$ is the fracture energy consumed for the free surface formation and K_0, k are two constants; $p_c(l,r)$ is defined by the union of the distributions (1) and (2). Physically, the function $K(l)$ means the following. If $K_0 = 3$, $k = -2$, it indicates that all the lost specific energy $f(r)$ would be spent only for the fragmentation with formation of new free surfaces, $S_c = 6l^2$, for each cube of material. Actually, one should take into consideration only a part of S_c due to the imperfect cohesion of blocks in rocks clearly recognizable [11] and, moreover, a part of the energy lost $f(r)$ is only expended directly in fragmentation or in fracture without disintegration (e.g., crack propagation without coalescence, etc.). Both these parts are not known even approximately, and we try to describe the ratio of these parts by the power function, where K_0, k are free parameters for future fitting. The boundaries of the regimes (2a-c), r_n, are determined from (2a) and (3) or (2c) and (3) by substituting $l_{\max} = l_{j+1}$ or $l_{\min} = l_j$ correspondingly. Meanwhile, r_1 and r_2 are obtained from the comprehensive analysis of the fine fragmentation (1) and (3), where now $K(l)$=constant and $l_{\min} = 0$. Note the quantum-continuous feature of the function $p_c(l,r)$ shows singularities as $r_n \to r_{3j-1}$; for example, $p_c(l,r)$ tends to the Dirac's distribution function for $m_j = 3$.

The differential distribution over the full fragmentation zone, $p(l)$, is the integral over the volume of $p_c(l,r) \neq 0$, evaluated between $r_{\min}$ and $r_{\max}$, these being the roots of the integer-algebraic equations followed from (2) and (3), i.e.:

$$p(l) = 4\pi R_0^3 \int_{r_{\min}}^{r_{\max}} r^2 p_c(l,r)\mathrm{d}r \qquad (4)$$

To derive the relative number of fragments, $N_i(l_i)$, (l_j contains among a set of l_i) for comparison with the nominal ones, N_i^0, and corresponding to the averaged explosion over the eight events [11], we introduce the intervals of integration, Δl_i, such that $N(\%) = 100\,N_i / N_\Sigma$.

$$N_i(l_i) = \int_{l_i - \Delta l_i}^{l_i + \Delta l_i} p(l)\,dl\,, \qquad N_\Sigma = \sum_i N_i \tag{5}$$

The Δl_i also are gently fitted, so that they become close to the half-length between l_i and l_{i+1}.

CALCULATION RESULTS

The fitting process carried out by the trial-and-error method shows essential sensibility to the variation of the governing parameters, K_0, k. This enable us to conclude the practical stability of the results obtained.

As the first approximation, the well-fitting numbers N_i and Δl_i, corresponding to the values $k = 1.4$, $K_0 = 0.00165$, $m_j = 3$ for *j*=1,..,6, and $m_7 = m_8 = 0.1$, are shown in Table 1 (numbers without brackets). The sizes l_i and the nominal data N_i^0 are taken from [11]. However, the maximum distances r_i turn out to be of order 10^3 instead of 10^2 [12, 13]. This of course can relate to an asteroid with the very weakly connected blocks, but to change the result in order to approach the earth conditions, let us assume the following. Firstly, the great difference in the block volumes l_j^3 and the fact that the empirical numbers of fragments N_i^0 grow with increasing l_i, lead to neglect very thin zones of the small-sized fragmentation ($l < 50mm$), which are hard to be highlighted with the help of a computer due to the well-known large-and-small numbers problem.

To clarify the situation, suppose that fragmentation occurs only in two characteristic sizes, $l_1 = 5\text{mm}$ and $l_2 = 3000\text{mm}$, and just $V_1 = 1\text{m}^3$ of volume is disintegrated into smaller particles. If the quality of the larger fragments is the same, the volume V_2 must be of $V_1 l_2^3 / l_1^3$ and occupies the sphere of radius ~400 m. Therefore this fact is due to a geometrical feature rather then to the model properties. Physically, the absence of the small particles, which only appear in the lab-scale experiments, can be explained by the large mutual displacements of the particles formed in the long-length wave under large compression. The great work of the friction forces transformed to heat is enough for the contact melting and then welding of these particles. Probably, the fine fragmentation observed in the natural experiments arises as a side action of the large-sized piece formation and their mutual collisions. By the way, in the small-sized fragment domain, the above mentioned maximums in the empirical distributions are slightly marked and sometimes disappear at all [11]. To keep the whole percentage, we ascribe the true value of $N_i = N_i^0$ for $l_i < 0.05\text{m}$ and calculate these numbers for the highest value of l_i beginning with $l_5 = 0.05\text{m}$. Secondly, we replace the constant K_0 by the function $K_0\left(1 + K_1 l + K_2 l^2\right)$ (here l is in meters).

The numbers in the brackets in Table 1 represent the fitting corresponds to the values $k = 1.5$, $K_0 = 3000$, $K_1 = 0.2$, $K_2 = 0.4$, $m_j = 0.5$ and the realistic fragmentation radius $r^* = 62.2$. Note that the influence of the quantities K_i, k remains very sharp as compared to others. For example, the variation of U_0 does not change dramatically the distribution, influencing only the values of distances r_i.

The cumulative number of fragments larger than a given size l, $N(l)$, is determined by integration of the function $p(l)$ from l to $\max l_i$. This cumulative distribution normalized by a value $N_0 = 10^4$ is plotted in Figure 1, in the double-logarithmic coordinate system. One can notice that this curve differs remarkably from a straight line that corresponds to the common fractal law; at least two straight lines, corresponding to a bi-fractality would have to be considered as observed in [8,9]. In particular, the weakly expressed maximums corresponding to the characteristic values l_j emerge.

l [mm]	5	10	20	30	50	70	100	140
$N_i^0(\%)$	4	2	3	3	5	4	5	7
$N(\%)$	5.6 (4.0)	2.4 (2.0)	3.7 (3.0)	3.0 (3.0)	4.6 (5.2)	4.3 (4.0)	5.2 (5.3)	6.9 (7.2)
Δl [mm]	1.1 (0.0)	1.9 (0.0)	0.6 (0.0)	4.5 (0.0)	2.0 (12.5)	9.0 (12.0)	24.0 (21.0)	7.5 (12.0)

l [mm]	200	300	500	700	1000	1400	2000	3000
$N_i^0(\%)$	7	10	13	9	12	7	5	2
$N(\%)$	7.0 (7.0)	9.7 (10.2)	13.1 (13.3)	8.6 (8.9)	12.0 (12.1)	7.0 (7.2)	5.1 (5.3)	1.9 (2.2)
Δl [mm]	30 (33)	108 (96)	51 (81)	158 (154)	92 (188)	225 (317)	67 (208)	67 (633)

Table 1

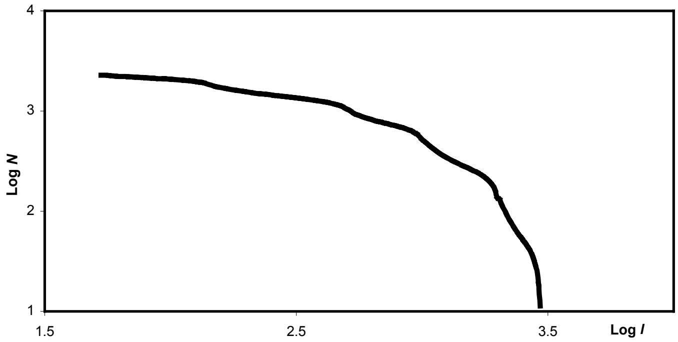

Figure 1: The cumulative fragment size distribution.

CONCLUSION

In this work, the attention was focused on the rock fragmentation resulting in the long-length shock wave action, which, in turn, is the aftereffect of a large explosion/impact. Unlike the lab-scale dynamic experiments [5,6] where only the fine fragmentation is evidenced, the block structure effect at the sizes $l > 5\mathrm{mm}$ dominates and, moreover, in such way that the larger fragment the greater its cumulative number [11]. The fragment size distribution assumed for a cell describes the fine crushing, when we employ the well-appropriate dynamic fragmentation model [9], or the block structure hierarchy disintegration. The latter is presented by a function with the quantum-continuous feature. Then the differential and cumulative distributions over the whole fragmentation volume are calculated. The free parameters of the model are determined by fitting with the empirical data [11]. To justify all physical conditions turns out to be the sophisticated task. Of course, in physics, many free parameters are not correct for any mathematical model, but, on the other hand, this reflects the complexity and uncertainty of the pattern of the fragmentation process. Thus, the analysis presented should be considered as one of the possible attempt on the way for a better understanding of the relation between the local and cumulative fragment size distributions at the large size scale. It appears that the multiscale dynamic fragmentation is a rather open question and there is much room for improvement of the fragment distribution statistic.

ACKNOWLEDGMENT

This work was partly supported by the Inter-branch Program of the Russian Academy of Sciences "Physics and mechanics of strongly-pressed matter and the problem on internal structure of the Earth and planets". The authors thank Prof. A. Carpinteri for the interesting scientific discussions.

REFERENCES

[1] Rittinger P.R., Lehrbuch der aufbereitungskunde, Berlin, 1867.

[2] Kick F., Das gesetz der proportionalen widerstände, Leipzig, 1885.

[3] Bond F.C., The third theory of comminution. *Mining Engineering.* **4**, 484-494, 1952.

[4] Béla Beke D. Principles of comminution, Publishing house of the Hungarian academic of sciences, Budapest, 1964.

[5] Fujiwara A., Kamimoto G., and Tsukamoto A., Destruction of basalt bodies by high-velocity impact, *Icarus.* **31,** 277-288, 1977.

[6] Takagi Y., Miltzutani H., and Kawakami S., Impact fragmentation experiments of basalt and pirophillites, *Icarus.* **94,** 283-298, 1984.

[7] Carpinteri A. and Pugno N., One-, two- and three-dimensional universal laws for fragmentation due to impact and explosion, *Journal of Applied Mechanics*. **69,** 854-856, 2002.

[8] Carpinteri A. and Pugno N., A fractal comminution approach to evaluate the drilling energy dissipation, *International Journal of Numerical and Analytical Methods in Geomechanics.* **26,** 499-513, 2002.

[9] Melosh H.J., Ryan E.V.,and Asphaud E., Dynamic fragmentation in impacts: hydrocode simulation of laboratory impacts, *Journal of Geophysical Research*. **97**. E9.14, 735-759, 1992.

[10] Grady D.E. and Kipp M.E., Dynamic Rock Fragmentation, Fracture Mechanics of Rock. Academic Press, 1987.

[11] Sadovskiy M.A., Bolkhovitinov L.G., and Pisarenko V.F., On property of discretion of rocks, *Physics of the Earth*. **12,** 3-18, 1982.

[12] Simonov I.V., The feasibility of using large impact to destroy a dangerous asteroid, *International Journal of Impact Engineering*. **27**(3), 293-315, 2002.

[13] Rodionov V.N., Adushkin V.V., Kostyuchenko V.N., Nikolaevskii V.N., Romashov V.N., and Tsvetkov V.I., Mechanical effect of underground explosion. Moscow-Nedra, 1971.

[14] Melosh H.J., Impact cratering: a geologic process. Oxford University Press, 1989.